Structure–Activity Relationships Among the Nitrogen Containing Bisphosphonates in Clinical Use and Other Analogues: Time-Dependent Inhibition of Human Farnesyl Pyrophosphate Synthase

James E. Dunford,*[,†,‡] Aaron A. Kwaasi,[†,‡] Michael J. Rogers,[§] Bobby L. Barnett,[||] Frank H. Ebetino,[▽] R. Graham G. Russell,[‡] Udo Oppermann,[†] and Kathryn L. Kavanagh[†,⊥]

Structural Genomics Consortium, The Botnar Research Centre, University of Oxford, Oxford OX3 7LD, United Kingdom, Nuffield Department of Orthopaedic Surgery, The Botnar Research Centre, University of Oxford, Institute of Musculoskeletal Sciences, Nuffield Orthopaedic Centre, Headington, Oxford OX3 7LD, United Kingdom, Bone and Musculoskeletal Research Programme, Institute of Medical Sciences, University of Aberdeen, Aberdeen AB25 2ZD, United Kingdom, Chemistry Department, University of Cincinnati, Cincinnati, Ohio 45221, Procter and Gamble Pharmaceuticals, Mason, Ohio 45040 and Department of Chemistry and Biochemistry, College of Natural Sciences, The University of Texas at Austin, Austin, Texas 78712

Received December 14, 2007

The nitrogen-containing bisphosphonates (N-BPs) are the main drugs currently used to treat diseases characterized by excessive bone resorption. The major molecular target of N-BPs is farnesylpyrophosphate synthase. N-BPs inhibit the enzyme by a mechanism that involves time dependent isomerization of the enzyme. We investigated features of N-BPs that confer maximal slow and tight-binding by quantifying the initial and final K_is and calculating the isomerization constant K_{isom} for many N-BPs. Disruption of the phosphonate−carbon−phosphonate backbone resulted in loss of potency and reduced K_{isom}. The lack of a hydroxyl group on the geminal carbon also reduced K_{isom}. The position of the nitrogen in the side chain was crucial to both K_i and K_{isom}. A correlation of K_{isom} and also final K_i with previously published in vivo potency reveals that the isomerization constant ($R = -0.77$, $p < 0.0001$) and the final inhibition of FPPS by N-BPs ($R = 0.74$, $p < 0.0001$) are closely linked to antiresorptive efficacy.

Introduction

Nitrogen-containing bisphosphonates (N-BPs[a]) are the current drugs of choice for the treatment of diseases characterized by excessive resorption of bone, such as postmenopausal osteoporosis, Paget's disease, or tumor-associated-osteolysis.[1–4] In the treatment of osteoporosis, the use of N-BPs reduces the fracture risk by 30–70% depending on the BP used and the type of fracture analyzed. Although BPs have been in clinical use for over 30 years, it is only within the past few years that it has become established that a major molecular target of the nitrogen containing bisphosphonates is the enzyme farnesylpyrophosphate synthase (FPPS)[5,6] within osteoclasts, the cells responsible for bone resorption. Moreover, besides the involvement of FPPS as a drug target for the treatment of bone diseases, FPPS and other enzymes of the mevalonate pathway have now been identified as potential targets in the treatment of diseases such as malaria, Chagas' disease, cryptosporidiosis, and leishmaniasis[7] caused by parasitic protozoans.

FPPS is a homodimeric enzyme that catalyzes the sequential condensation of the 5-carbon allylic substrate, dimethylallyl pyrophosphate (DMAPP), with two molecules of the 5-carbon isopentenyl pyrophosphate (IPP) to first form C10 geranylpyrophosphate (GPP) and ultimately the C15 farnesyl pyrophosphate (FPP). This isoprenoid is utilized in the production of many other metabolites such as cholesterol, heme, ubiquinone, geranylgeranyl pyrophosphate, and for the prenylation of proteins. Inhibition of FPPS leads to a diminished post-translational prenylation of small GTPase proteins, important in osteoclast cell function and survival, which forms the basis of antiresorptive therapy with N-BPs.[8,9] Recent structure determinations of N-BPs complexed to human, trypanosomal, and bacterial FPPS orthologs have revealed the mode of binding.[10–14] The phosphonate groups of the N-BP coordinate via Mg ions with the aspartate-rich motifs of the enzyme, which are associated with binding the pyrophosphate groups of the allylic (DMAPP/GPP) substrate (Figure 1). The nitrogen in the R2 side-chain of the potent N-BP (Figure 2 and Table 1) is known to be critical for this effect[15] and is properly oriented for hydrogen bonding with the hydroxyl of residue Thr201 and the carbonyl oxygen of Lys200 in the active site of the enzyme (Figure 1). The putative role of these residues is to stabilize a carbocation intermediate formed during the condensation of the two substrates[16] and the cationic side chain of the N-BP is proposed to act as a transition state analogue.[17]

A time-dependent inhibition of FPPS was initially reported for alendronate (ALN;[6] Table 1), followed up by a more detailed analysis of the inhibition mechanism by risedronate (RIS; Table 1) and zoledronate (ZOL;[10] Table 1). These N-BPs are competitive inhibitors with regard to the allylic substrate DMAPP/GPP and uncompetitive inhibitors with regard to IPP. These clinically important N-BPs have initial inhibition constants (K_i) in the nM range and become even

* To whom correspondence should be addressed. Nuffield Department of Orthopedic Surgery, The Botnar Research Centre, University of Oxford, Institute of Musculoskeletal Sciences, Nuffield Orthopedic Centre, Headington, Oxford OX3 7LD, U.K. Tel.: +44 (0)1865 227658. Fax: +44 (0)1865 227966. E-mail: james.dunford@ndos.ox.ac.uk.

† Structural Genomics Consortium, University of Oxford.

‡ Nuffield Department of Orthopaedic Surgery, University of Oxford.

§ Institute of Medical Sciences, University of Aberdeen.

|| University of Cincinnati.

▽ Procter & Gamble Pharmaceuticals.

⊥ The University of Texas at Austin.

[a] Abbreviations: FPPS, farnesyl pyrophosphate synthase; N-BPs, nitrogen-containing bisphosphonates; IPP, isopentenyl pyrophosphate; DMAPP, dimethylallyl pyrophosphate; FPP, farnesyl pyrophosphate; GPP, geranyl pyrophosphate; LED, lowest effective dose; ALN, alendronate; IBA, ibandronate; NER, neridronate; PAM, pamidronate; RIS, risedronate; ZOL, zoledronate; APHBP, aminopentane hydroxyl bisphosphonate; BP, Bisphosphonate.

10.1021/jm7015733 CCC: $40.75
Published on Web 03/08/2008

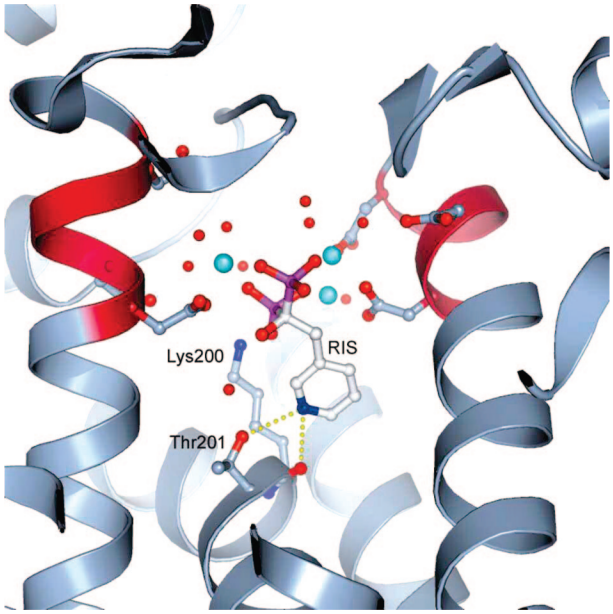

Figure 1. Diagram showing the binding of RIS to FPPS; α-Carbon trace of the active site of human FPPS with RIS bound. Regions containing the aspartate rich motifs are shown in dark red, magnesiums and waters are shown as cyan and red spheres, respectively, and residues within 3.2 A of Mg or RIS are depicted in ball-and-stick representation. Polar interactions between the bisphosphonate nitrogen and Lys200 and Thr201 are indicated by dashed yellow lines. Data from PDB ID 1YV5.[10]

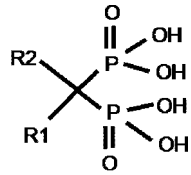

Figure 2. General structure of a bisphosphonate. R1 is usually a hydroxyl, and the structure of R2 varies widely and is responsible for differences in potency.

more potent with time, defining them as "slow, tight-binding" inhibitors.[18,19] The time-dependent inhibition is widely interpreted as being due to an isomerization of the enzyme–inhibitor complex,[19] which produces more potent inhibition. There are other explanations for slow binding, chiefly that the inhibitor is simply slow to bind to the enzyme, or that after binding the inhibitor then goes on to slowly form a covalent link to the enzyme. However, in support of the isomerization theory for slow binding, evidence from crystal structures of the enzyme show that a considerable structural rearrangement of the enzyme occurs upon initial binding of substrate or a bisphosphonate to the DMAPP/GPP site.[10,11] The α-helices that comprise the core and line the active site of the enzyme move closer together to decrease the size of the internal cavity while also forming the IPP binding site.[10] IPP binding induces a second isomerization step, which promotes active-site closure by the C-terminus of the enzyme. Also, no covalent linkage of the BP to the enzyme has been observed, thus, it is likely that the time dependence of the inhibition is due to subtle rearrangements of the enzyme induced upon inhibitor binding.

Despite this advance in knowledge, the exact mechanism of inhibition of the enzyme by these compounds is still not fully understood, and in particular, comprehensive structure–activity relationships among the BPs as inhibitors of the human or mammalian enzyme have not been determined. The aim of this study was, therefore, to investigate the time-dependent mechanism of inhibition for clinically relevant N-BPs and some structural analogs and to compare their potency as FPPS inhibitors to their efficacy in vivo as inhibitors of bone resorption.

Table 1[a]

	Compound	R1	R2		Compound	R1	R2
1	Pyrophosphate		O_3P-O-PO_3	10	NE58051	OH	
2	Pamidronate	OH		11	NE58022	OH	
3	Alendronate	OH		12	NE58043	H	
4	Neridronate	OH		13	NE10575	OH	
5	YM-175	H		14	NE58027	OH	
6	Ibandronate	OH		15	NE58034	H	
7	Zoledronate	OH		16	NE58018	OH	
8	Risedronate	OH		17	NE97221	H	
9	APHBP	OH		18	NE21650	OH	
	Phosphonocarboxylate				Monophosphinate		
19	NE10790	OH	*	20	NE10788	H	*
	Compound	R1	R2		Compound	R1	R2
21	NE11808	H		24	NE97220	H	
22	NE11809	H		25	NE58062	H	
23	NE11807	H					
	Methyl-phosphinate analogues of **24** (NE97220)						
26	NE58029	H	*	27	NE58052	H	*

[a] Clinically relevant BP (**2**−**8**) are either in clinical use or have been used in clinical trials[4] (**10**−**27**).[8,15,21,27,31] *Complete structure.

Results

Farnesyl pyrophosphate synthase inhibition data was generated as described and was used to calculate the bisphosphonate concentration that gives 50% inhibition (IC_{50}) for each compound, both in initial rate experiments and also after a 10 min preincubation time with the N-BP (Figure 3 and Table 2). Clear differences in initial and final inhibition were observed, with most bisphosphonates becoming more potent with preincubation. Incubation time periods greater than 10 min did not significantly

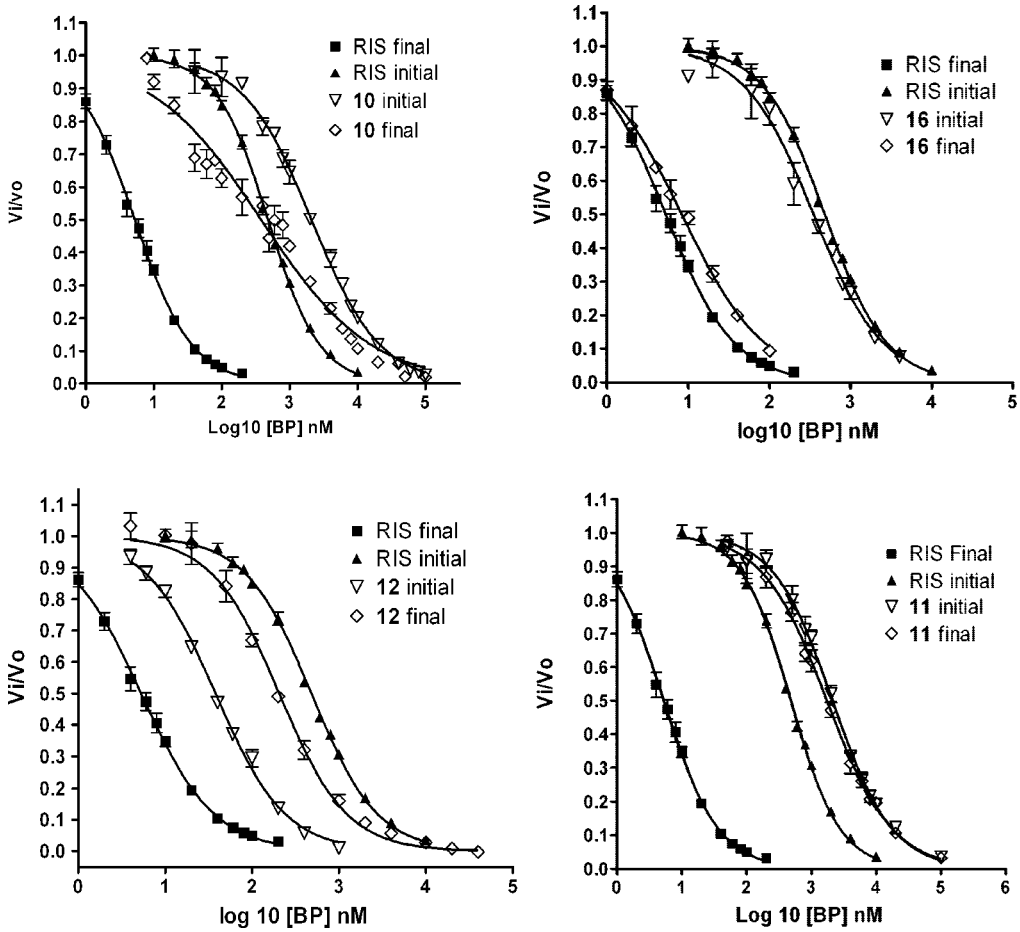

Figure 3. Plot of inhibition data showing changes in potency of RIS and associated compounds with a 10 min preincubation of enzyme and inhibitor.

increase the inhibition. A plot of K_i* against K_{isom} (Figure 4 and Table 3) reveals a linear relationship between final K_i* and K_{isom}, suggesting that in general the compounds with the lowest final inhibition had the greatest K_{isom}, although there are exceptions, such as **24**, which has a low K_i*, but also a relatively low K_{isom}.

Changes to the Phosphonate−Carbon−Phosphonate (O−P−C−P−O) Backbone. The O−P−C−P−O backbone of the bisphosphonates is critical for binding to the enzyme. As expected, the complete removal of a phosphonate group from RIS (**20**) results in almost complete loss of inhibition with a final IC_{50} of 824 μM compared to 5.7 nM for RIS itself. The replacement of one of the phosphonate groups with a carboxyl group (**19**) resulted in a 44000-fold decrease in potency relative to the parent compound RIS and an initial IC_{50} of 467 μM and a final IC_{50} of 250 μM. Although a shift in IC_{50} is observed with time, the final value is approximately 25 times the concentration of each of the substrates available to the enzyme and indicates that the inhibition is only weakly competitive. In all the above cases, inhibition was found to be less than that achieved by pyrophosphate, one of the natural products of the enzyme. Substitution of a hydroxyl with a methyl group on one of the phosphonates to form a phosphono-phosphinic analog (i.e., **26**) increases the IC_{50} from the parent compound (**24**), whereas a bisphosphinic analog (**27**) no longer inhibits even at high concentrations

Inhibition by Risedronate Analogues. The analogues of RIS vary considerably in potency, with small changes to the structure of the inhibitors (Table 3) causing large differences in potency (Table 1).

Substitution of the hydroxyl at the R1 position of the geminal carbon of RIS with hydrogen to give the compound **12** leads to an increased initial inhibition relative to RIS but a decreased final inhibition. This is also the case with the pairs of compounds **16/17** and **14/15**, where the BP lacking the hydroxyl at the R1 position is a slightly better initial inhibitor but, ultimately, the weaker final inhibitor.

Any changes to the ring nitrogen of RIS resulted in decreased inhibition. In particular, the phenyl analogue of RIS with no heterocyclic ring nitrogen (**11**) has an initial IC_{50} of 2000 nM (compared to 450 nM for RIS) and completely lacks the time-dependent increase in potency observed with RIS. Compound **10**, which has an additional carbon in the side-chain that increases the distance between the nitrogen and the phosphonate group, also had a reduced initial inhibition relative to RIS, with the IC_{50} increasing to 2100 nM. This analogue is still capable of producing a time-dependent shift in inhibition, although the final IC_{50} shows that it is weaker in comparison to the parent compound. Addition of a methyl group to the nitrogen to produce a pyridinium structure (giving the nitrogen a positive charge and adding steric bulk, **13**) also increased the initial IC_{50} relative to RIS but also reduced the potency after preincubation. This was again observed when the nitrogen was present as an ortho amino group attached to the phenyl ring rather than a heterocyclic ring nitrogen (**18**). The position of the nitrogen within the ring also influenced potency. Thus, having the nitrogen in the 2 rather than the 3 position in the ring (**16**) resulted in a marginal increase in initial potency, but ultimately resulted in weaker final inhibition with final IC_{50}s of 5.7 nM for RIS and 9.2 nM for **16** ($p < 0.001$, Student's *t*-test). When

the pyridyl ring structure of **16** was compared to its saturated piperidine counterpart (**14**), both initial and final potency was decreased.

Inhibition constant (K_i) values were calculated from the initial inhibited rate data, where the experiment was initiated by the addition of enzyme, and the preincubated rate data, where the enzyme was preincubated with BP and the reaction started by the addition of substrate. The constants were then corrected for the allylic (GPP) substrate affinity of the enzyme (Km_{GPP}) and also GPP concentration.[18] The K_i values calculated for the analogues of RIS (Table 3) showed a similar pattern of inhibition to that described by the IC_{50} values (Table 2).

The shift in potency from the initial competitive state to the final inhibitory state can be quantified by an isomerization constant, K_{isom},[10,18,19] which can be calculated from K_i and K_i*. This constant indicates the reversibility of the isomerization; the larger the number the more the equilibrium lies to the right (the isomerized state). It also implies that the compounds with higher K_{isom} will inhibit the enzyme for longer and be less reversible.

All the analogues of RIS that were analyzed showed decreased isomerization constants relative to the parent compound (Table 3). For both of the pairs, RIS/**12** and **16/17**, the lack of the hydroxyl on the geminal carbon resulted in large decreases, greater than 10-fold, in the isomerization constant relative to the parent compound. Also, any modification to the position of the nitrogen relative to the phosphonate resulted in a reduced K_{isom}. Even the difference of having the nitrogen in the 2 compared to the 3 position (**16**) results in an approximate 3-fold reduction in the ability of the inhibitor to hold the enzyme–inhibitor complex in the isomerized state.

Inhibition by Other Nonclinical NBPs. Compounds **21/22** are a pair of compounds that have been used in the past to demonstrate how small changes in structure can lead to large changes in potency.[5] Compound **21** was demonstrated to be a potent compound (Tables 2 and 3) and the crystal structure of **21** bound to *T. brucei* FPPS shows that it binds with the ring essentially coplanar to RIS or ZOL, but with the ring nitrogen shifted over 1.4–1.7 Å compared to the human FPPS complexes.[20] The potency of **21** is postulated to be the result of extensive charge delocalization of the amidinium side chain and charge complementarity within the FPPS active site. However, when a methyl group is added to the ring structure of **21** to form **22**, any time-dependent increase in inhibition is abolished and the potency is vastly reduced. Comparison of modeling results for **22** and crystallographically determined FPPS/N-BP structures suggests a poor agreement in binding with respect to the nitrogen and ring orientation.[20] Similar to **21** is **23**, which has one carbon less in the R2 side chain (Table 3). For the pair of BPs, **21/23**, this change in length of the R2 side chain, which can affect potency, as seen with the comparison of **10** and **8**, causes no differences in final potency and only a minor change in isomerization constant. This may be because the pyridyl amidinium nitrogen moiety may orient in a similar manner to the critical nitrogen of RIS and ZOL. The further addition of a methyl group to the ring structure of **23** to form **24** leads to increased initial and final potency, with the isomerization constant being approximately the same as for the parent compound. However, partial reduction of the ring leaving only a C=N double bond to give **25** leads to a 7-fold increase in initial IC_{50}, while the final IC_{50} increased 1.7-fold (Table 2). This is reflected in an approximate 8.5-fold increase in isomerization constant (Table 3).

Table 2. IC_{50} Values for the Inhibition of FPP Synthase by Bisphosphonates[a]

cmpd	initial IC_{50} (nM)	final IC_{50} (nM)
1	243 ± 21.5 μM	181 ± 19.1 μM
2	1932 ± 152.6	353.2 ± 32.1
3	2249 ± 180	260.0 ± 19.6
4	2427 ± 147	388.2 ± 23
5	365.6 ± 32	61.1 ± 5.1
6	1052 ± 55.1	25.4 ± 1.57
7	475.3 ± 18.3[(1)]	4.1 ± 0.22[(1)]
8	452.9 ± 16.6[(1)]	5.7 ± 0.54[(1)]
9	1079 ± 82.1	298.5 ± 36.6
10	2113 ± 188	337.3 ± 77
11	2099 ± 130.6	1626 ± 192
12	173.4 ± 10.5	32.6 ± 2
13	1706 ± 334	19.6 ± 3.4
14	591.6 ± 91.6	13.7 ± 0.9
15	869.0 ± 77.0	23.8 ± 2.5
16	349.1 ± 22.7	9.2 ± 0.96
17	258.8 ± 21.2	30.4 ± 2.0
18	370.7 ± 14.3	21.6 ± 2.8
19	467 ± 70 μM	254 ± 21 μM
20	ND	824 ± 21 μM
21	190.1 ± 22.5	15.0 ± 3.3
22	988.6 ± 50.6	734.5 ± 48.9
23	166.0 ± 15.3	11.7 ± 3.1
24	75.2 ± 4.6	6.2 ± 1.45
25	540.8 ± 16.9	10.3 ± 0.5
26	1892 ± 231	61.4 ± 0.5
27	ND (>10 mM)	330 ± 85 μM

[a] $n > 3$. [(1)]From Kavanagh et al.[10] ND = not determined.

Inhibition by Clinically Relevant N-BPs. The IC_{50} data for the clinically relevant bisphosphonates (as defined in Table 1) showed they were all capable of time-dependent increases in inhibition of FPPS. For the initial IC_{50}s determined without preincubation YM-175, Ris, and ZOL were the most potent with IC_{50}s in the region of 360 to 450 nM. IBA, PAM, ALN, and NER were distinctly less potent with initial IC_{50}s of 1000, 1900, 2250, and 2400 nM, respectively (Table 2). Preincubation of the N-BP with FPPS resulted in a decrease in IC_{50}. ZOL was the most potent bisphosphonate tested with a preincubated IC_{50} of 4.1 nM, with Ris, IBA, and YM-175 at 5.7, 25, and 61 nM, respectively. In this present study, ALN, PAM, and NER were the least potent, all with very similar IC_{50}s of 260, 353, and 390 nM. Expressing this data in the form of K_i resulted in similar values and did not change the order of potency of these compounds (Figure 5A). The isomerization constants for the clinically relevant N-BPs revealed that ZOL is the best compound at holding the enzyme in the isomerized state, followed by RIS and IBA. ALN, YM-175, and NER have similar values, while PAM has the lowest isomerization constant of all the clinically relevant compounds (Figure 5B).

Correlation of LED with K_i* and Isomerization Constant. The order of inhibitory potency for the clinically relevant N-BPs of FPPS generally ranks in a similar order to the potency of the compounds in vivo as measured using the Schenk assay in growing rats.[8,15,21] Only ALN and PAM showed a different pattern of inhibition with PAM and ALN being equivalent in vitro, while ALN is considerably more potent in vivo. The comparison of the LED with K_i* for all the compounds for which the LEDs are published shows a direct correlation of enzyme inhibition with potency in vivo ($r = 0.74$, $p < 0.0001$; Figure 6A). However, this analysis shows IBA, ALN, and **13** to be more potent in vivo than their overall ability to inhibit FPPS would suggest. This could be due to other relevant properties that affect in vivo potency, such as bone-binding affinity, differences in cellular uptake, or the possibility that there are other currently unknown targets for inhibition.[22]

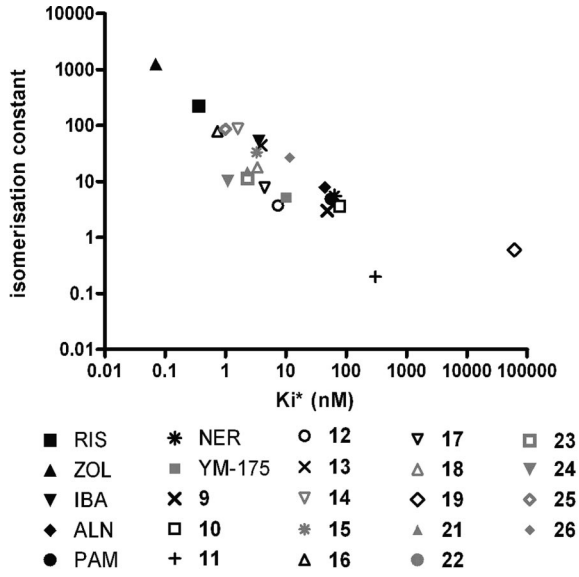

Figure 4. Relationship between K_i* and K_{isom}.

The relationship between LED and isomerization constant shows a significant negative association (Spearman correlation $r = -0.77$, $p < 0.0001$), (Figure 6B), that is, the higher the isomerization constant, the lower the LED in vivo and the more potent the bisphosphonate.

Time-Dependent Inhibition of FPPS by Risedronate. The inhibition of FPPS by RIS increases over time as shown in Figure 7A. We studied the time dependence of the interaction of RIS and FPPS by preincubating the enzyme with inhibitor and initiating the reaction by the addition of substrate (Figure 7B). As the initial competition stage of the inhibition to form an enzyme–inhibitor complex is very rapid, the increase in inhibition that is seen following preincubation with N-BP is due to the isomerization of the enzyme–inhibitor complex. It is possible to calculate k_5 by fitting this data to the equation for exponential decay.[18] For RIS, this was found to be 0.49 ± 0.07 min^{-1}. In experiments in which enzyme was allowed to equilibrate with RIS followed by a reaction timecourse, a "reversed progress curve", it was established that the rate of reaction remained unchanged until substrate became limiting, after about 5 min. This indicates that after the addition of substrate to the reaction there is no measurable reactivation of the enzyme, at least over the time of the assay. The preincubation experiments (Figure 7B) were performed in the absence of IPP, so the preincubated enzyme–inhibitor complex would not have IPP bound. No significant difference was observed in the inhibition with preincubation in the presence of IPP (10 μM; data not shown). As the assay is performed in the presence of IPP, and binding of IPP to the enzyme–inhibitor complex is presumed to occur rapidly, its effect cannot be measured using this assay.

As described above, we have calculated k_5 for RIS, which allows us to calculate k_6 from eq 2, which for RIS is 0.0022 min^{-1}. Thus, the half-life for the reversal of the enzyme−RIS isomerized complex is calculated to be approximately 5 h.

Discussion

We have examined in detail the structure–activity relationships of N-BPs and the inhibition of FPP synthase in light of the time-dependent nature of the inhibition. Time-dependent inhibition is usually a result of an enzyme isomerization event,[19] and we and others[10,11] have previously shown that the enzyme undergoes a structural rearrangement on inhibitor binding. The application of these slow-binding theories has allowed us to gain novel insight into the N-BP inhibition of FPP synthase.

Role of the Phosphonate Groups. Conserved sequences in FPPS that have been known to be important in catalysis include the aspartate-rich fingerprint regions that are involved with coordinating the substrate phosphate moieties via divalent metal ions.[23,24] We have previously shown the importance of these residues for the interaction of the enzyme and bisphosphonate.[10] It is clear from our current results that the loss of these interactions either by removal or replacement of a phosphonate with a carboxylic acid as in the case of **20/19** or by a phosphinic acid (**26**) leads to a huge loss in potency and a total abrogation of the ability to hold the enzyme–inhibitor in an isomerized state. In fact, given that the substrate concentration is 10 μM and the IC_{50} values are greater than 250 μM, it could be argued that these compounds are not inhibitors of FPPS at all and the inhibition seen could be attributed to sequestration of the Mg in the assay buffer by the bisphosphonate. The anchoring of the bisphosphonate in the active site by the magnesium-dependent aspartate−phosphonate interactions is thus a vital component in the inhibitor binding and the subsequent isomerization of the enzyme–inhibitor complex.

Role of the Hydroxyl Moiety. The hydroxyl at the bisphosphonate R1 position has been shown to form a water-mediated interaction with Gln240 and is also in close proximity to Asp243, which coordinates with magnesium.[11] An analogue of RIS with no hydroxyl group, **12**, initially inhibits better than the parent compound, but lack of the hydroxyl at R1 ultimately reduces the ability of the N-BP to hold the complex in the isomerized state. The same also occurs with **16/14** and their deshydroxy analogues **17/15**. The absence of the hydroxyl would therefore appear to initially make the N-BP a better competitive inhibitor, able to fit into the open active site more easily. Invariably, the N-BPs with a hydroxyl at R1 are the better final inhibitors, which suggests that interactions perhaps mediated by the hydroxyl further stabilize the isomerized state. Also, inspection of the FPPS/ZOL-IPP crystal structure suggests that the presence of the hydroxyl may improve the packing with IPP and that compounds lacking a hydroxyl may form a looser ternary complex (i.e., would be destabilized).

Role of the Nitrogen Moiety. The recently determined crystal structures of FPPS with N-BPs bound reveal that the nitrogen of the N-BP can form hydrogen bonds with Thr201 and the carbonyl of Lys200 (Figure 1). Changing the position of the nitrogen relative to the bisphosphonate group in the analogues of RIS (e.g., **10** and **16**) leads to a movement of the N away from Thr201 and Lys200 and would therefore disrupt the hydrogen bond geometry seen in the crystal structure. For compound **10**, this has been demonstrated by crystallography to lack appropriate orientation of the nitrogen within the GPP site.[25] This usually leads to a loss in initial potency and also to a reduced ability to hold the enzyme–inhibitor complex in the isomerized state. Even a small change in the nitrogen position, such as in **16**, leads to a decrease in potency and isomerization constant. In this case, the reduction in overall potency and isomerization constant is most likely to be a result of the reduced interaction of the nitrogen in the 2 position of the ring with Thr201 and Lys200 inferred from structural studies.[10] The phenyl analogue that lacks the nitrogen (**11**) displays the complete loss of slow-binding kinetics and an overall reduction in potency, an indication that the nitrogen has a role to play in the initial competitive phase of the inhibition as well as in stabilizing the final isomerized state. There could be two further

Table 3[a]

cmpd	initial K_i (nM)	final K_i* (nM)	K_{isom}	LED (mg P/Kg)
Kinetic Constants for the Inhibition of FPP Synthase by Pyrophosphate and Clinical Relevant and Aminoalkyl Bisphosphonates				
1	40.5 ± 3.9 μM	29.8 ± 3.2 μM	0.4	NA
2	331.4 ± 33.8	55.9 ± 6.1	4.9	0.03
3	393.1 ± 24.7	44.2 ± 3.4	7.9	0.001
4	415.7 ± 24.1	63.5 ± 5.3	5.5	0.01
5	62.4 ± 5.2	10.0 ± 0.9	5.2	0.001
6	195 ± 13.8	3.6 ± 0.3	52.9	0.0001
7	85.9 ± 3	0.07 ± 0.01[b]	1244	0.0001
8	82.2 ± 2.2	0.36 ± 0.06[b]	226	0.0003
9	194.1 ± 14.4	48.2 ± 5.6	3.0	NA
Kinetic Constants for the Inhibition of FPP Synthase by Analogues of RIS (**8**)				
10	362.6 ± 15.6	78.0 ± 8.2	3.6	1
11	367.9 ± 16	302.6 ± 17.6	0.2	0.1
12	34.76 ± 2.1	7.4 ± 0.2	3.7	0.01
13	177 ± 18.2	3.9 ± 0.3	44	0.0001
14	136.7 ± 23.1	1.6 ± 0.1	87.1	0.001
15	112.2 ± 10.9	3.28 ± 0.25	33.2	NA
16	59.3 ± 3.6	0.74 ± 0.12	78.9	0.001
17	38.95 ± 2.0	4.45 ± 0.18	7.8	0.01
18	64.6 ± 5.8	3.4 ± 0.3	17.8	0.001
Phosphonocarboxylate				
19	97.5 ± 25 μM[c]	61.0 ± 5.7 μM[c]	0.6	0.3
Monophosphinate				
20	ND	128.3 ± 23 μM[c]	ND	NA
Kinetic Constants for the Inhibition of FPP Synthase by Other Bisphosphonates				
21	36.9 ± 4.3	2.3 ± 0.3	15.1	0.01
22	155.4 ± 17.7	196.2 ± 18.6	−0.2	1.0
23	29.1 ± 1.8	2.3 ± 0.2	11.5	0.01
24	12.1 ± 2.4	1.09 ± 0.1	10.2	0.001
25	86.3 ± 8.9	1.0 ± 0.07	86	0.0003
Methyl-phosphinate Analogues of **24**				
26	319.7 ± 28.2	11.6 ± 0.7	26.6	1.0
27	ND >4 × 10^6	93.0 ± 8.6 μM	ND	inactive

[a] K_i and K_i* calculated using eq 1, $R^2 > 0.95$, $n > 3$, and corrected for KmGPP and [GPP]. NA = not available, ND = not determined. [b] From Kavanagh et al.[10] The in vivo LED is for inhibition of bone resorption in rats.[8,15,21] Compound **1** has not been shown to inhibit bone resorption in vitro or in vivo.[32] [c] $R^2 > 0.7$, $n = 4$.

features that come into play when comparing RIS and the phenyl analogue: protonation and symmetry of the side chain. NMR studies and quantum mechanical calculations show that N-BPs bind to FPPS in their protonated form.[26] At neutral pH the majority of RIS in solution is not protonated, hence, the enzyme must either select for the protonated form or RIS must pick up a proton once in the active site. This is not the case with the phenyl analogue, as it does not carry a +1 charge. The phenyl analogue is also symmetric and the ring can only bind in one orientation, while RIS could initially bind with the ring in two different orientations. Rotation of the pyridyl ring toward the optimal RIS binding pose and the nitrogen protonation state may thus contribute to the time-dependence of inhibition.

Clinically Relevant N-BPs. Our results are consistent with previously published data for the overall potency of clinically relevant N-BPs.[5,6] In the crystal structures,[11] the nitrogen of PAM and IBA do not form interactions with Thr201 or Lys200, as opposed to RIS and ZOL, yet both are capable of forming a tightly bound isomerized complex. This suggests that other residues besides Thr201 and Lys200 in the active site interact with the R2 side-chain nitrogen. Indeed, PAM is in H-bond distance to Tyr204, and this interaction might allow for the tightly bound complex to form. IBA is a considerably better inhibitor than PAM and also has a much higher isomerization constant. The hydrophobic interactions of the long IBA pentyl side chain may also aid in stabilizing the closed conformation.

Here we show that the overall ability of an N-BP to inhibit FPPS is closely linked to its potency to inhibit bone resorption in vivo. The ability of an N-BP to hold the FPPS−inhibitor complex in the isomerized state, as measured by the isomerization constant K_{isom} is also linked to the final potency, with the most potent N-BPs both in vivo and in vitro having the highest isomerization constants. The isomerization constant is an equilibrium constant that does not give any indication of the time involved to reach equilibrium. The results with RIS indicate that the off rate, k_6, is likely to be in the order of many hours for the most potent compounds. It is now clear that two distinct isomerization steps occur along the path of ligand binding to FPPS, the first being initial N-BP binding to the DMAPP cavity and tightening of the active site (ref 10 and this study), followed by IPP binding and closure of the active site. In addition, Rondeau et al.[11] suggest that the second isomerization step, the IPP binding followed by the stabilization of the C-terminus is also likely to help stabilize the enzyme–inhibitor complex. We have found little difference in the establishment of the enzyme–inhibitor complex in the presence or absence of IPP, but as the enzyme is already inhibited and IPP binding is presumed to occur rapidly, its effects on the inhibition are unlikely to be observed in the experiments described. The IPP binding may well have some effect on prolonging the inhibition, but regardless of this, we have calculated that the inhibition of FPPS by a potent N-BP alone is likely to take many hours to reverse.

In conclusion, we have shown that the inhibition of FPPS by N-BPs has a time-dependent component consistent with an isomerization of the enzyme–inhibitor complex. Such an

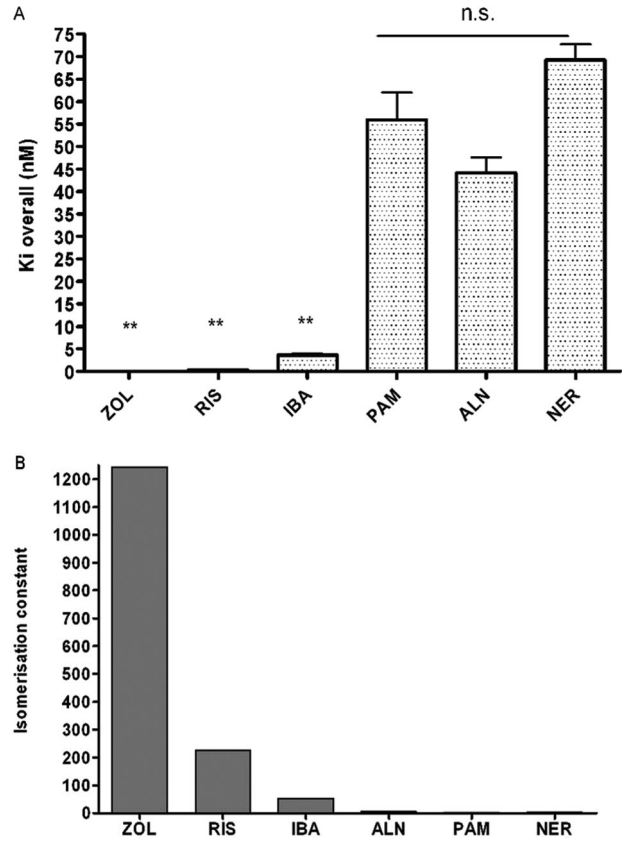

Figure 5. (A) Comparison of final K_i for clinically relevant N-BPs. K_i was calculated from preincubated enzyme inhibition data fitted to eq 1, $n > 3$, $R^2 > 0.95$. $^{**}p < 0.01$. Student's t-test). (B) Comparison of isomerization constant, K_{isom}, for clinically relevant BPs.

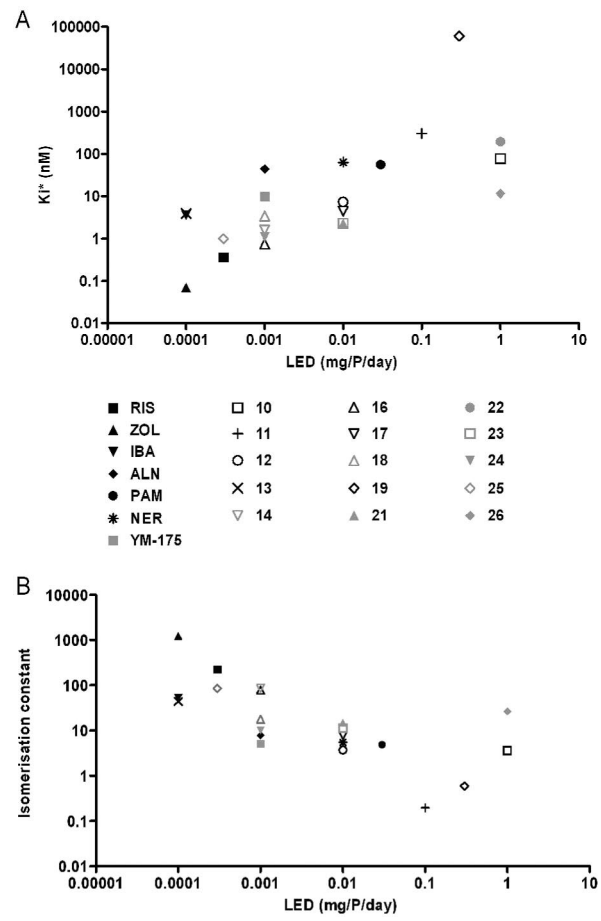

Figure 6. (A) Relationship between K_i* and LED (lowest effective dose (mg P/kg)); Spearman $r = 0.74$, $p < 0.0001$, Spearman's correlation. (B) Relationship between K_{isom} and LED; Spearman $r = -0.77$, $p < 0.0001$, Spearman's correlation.

isomerization has been observed in the enzyme in structural studies, and it seems highly likely that these two events are closely related, although it remains unclear as to the exact mechanism of the time-dependent inhibition observed in this system. Previous structure–activity analyses do not take the slow-binding mechanism into account. Interaction of the N-BP phosphonates and hydroxyl moiety with the aspartate-rich regions of the enzyme is essential for the formation of the final, tightly bound state, and the presence and position of the nitrogen relative to the bisphosphonate group is critical for maximum inhibition. It is apparent that the overall ability of the N-BPs to inhibit the enzyme is very closely linked to their in vivo potency and that the ability of an N-BP to hold the enzyme in the isomerized state also plays a crucial role in the overall potency.

Experimental Section

All bisphosphonates were obtained from Procter and Gamble Pharmaceuticals,[8,15,21,27] except pamidronate and alendronate, which were from Sigma. Unlabeled IPP and GPP were from Echelon biosciences,[14] and labeled IPP was obtained from Amersham.

Expression and Purification of Recombinant Human FPPS. An expression construct encoding human FPPS (gi 61680822) as N-terminally His_6-tagged fusion protein with a TEV cleavage site was expressed in *E. coli* BL21(DE3).[10] Cells were lysed using a high pressure cell disruptor, and the protein was purified to apparent homogeneity using Ni-NTA resin (Qiagen). Gel filtration chromatography was then performed using a Superdex 200 column (GE/Amersham).

FPP Synthase Assay. FPP synthase activity was measured by the method of Reed and Rilling[28] with modifications. For kinetic analysis, 40 ng (1 pmol) of pure FPP synthase were assayed in a final volume of 100 μL buffer containing 50 mM Tris pH 7.7, 2 mM $MgCl_2$, 0.5 mM TCEP, and 20 μg/mL BSA. The concentrations of substrates, GPP, and IPP (14C-IPP, 400 KBq/μmol) were 10 μM each in the standard reaction. Reactions also contained the appropriate concentration of N-BP. Reactions were started with the addition of enzyme at 2 μg/mL in enzyme dilution buffer (10 mM HEPES pH 7.5, 500 mM NaCl, 5% glycerol, 2 mM TCEP, 20 μg/mL BSA) and allowed to proceed for an appropriate period of time at 37 °C. Where a preincubation of the enzyme with the inhibitor was required, the appropriate quantity of enzyme was incubated with inhibitor in reaction buffer in a volume of 80 μL. After 10 min, 20 μL of substrate in water was added to start the reaction and also bring the inhibitor and substrate to the final desired concentrations. Reactions were timed such that a maximum of 10% of the available substrate was used. Assays were terminated by the addition of 0.2 mL of concd HCl/methanol (1:4) and incubated for 10 min at 37 °C. The reaction mixtures were then extracted with 0.4 mL of ligroin to separate reaction products from unused substrate and, after thorough mixing, 0.2 mL of the ligroin upper phase was combined with 4 mL of general purpose scintillant. The radioactivity was then counted using a Packard Tricarb 1900CA scintillation counter.

Kinetic Models and Calculation of Constants. Under certain circumstances, it is possible to establish conditions under which the slow binding phenomena can be observed. At high concentrations of inhibitor and low, subsaturating substrate concentrations, the time-dependent inhibition of FPPS by RIS can be observed (see below). This behavior is characteristic of slow-binding inhibitors and shows a time-dependent increase in inhibition. Determination of slow-binding ligand characteristics were analyzed based on the equation developed by Morrison and Copeland.[18,29,30] Inhibition constants (initial K_i, final K_i*, and isomerization constants) were

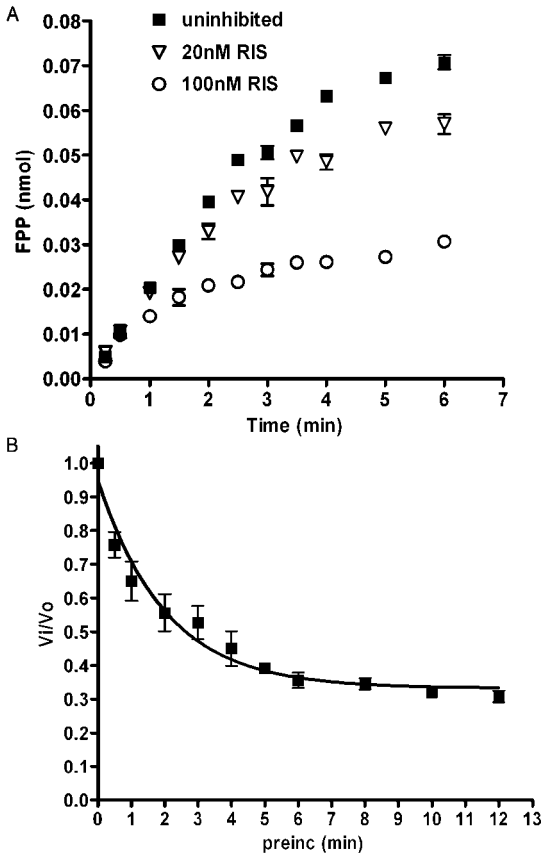

Figure 7. (A) Time-dependent inhibition of FPP synthase. Reactions were initiated by the addition of enzyme in the presence or absence of inhibitor and allowed to proceed for the indicated period of time. Reactions were performed with 2 μM each of GPP and IPP. (B) Time-dependent inhibition of FPP synthase. Enzyme (1 pmol) was preincubated for the specified period of time with 1 pmol RIS. Reactions were initiated by the addition of 10 μM of each substrate and were terminated after 3 min. Data were fitted to the equation for exponential decay.[18] $R^2 = 0.9$, $n = 4$.

calculated as described.[10] Briefly, enzyme and inhibitor experiments that showed strong inhibition, defined as having an initial inhibition constant K_i or preincubated inhibition constant K_i* no greater than 10 μM (1000× the enzyme concentration),[18,30] were fitted to Morrison's equation, also equivalent to an active site titration.[18]

$$\frac{Vi}{Vo} = 1 - \frac{\left([E] + [I] + K_i{*}^{app}\right) - \sqrt{\left([E] + [I] + K_i{*}^{app}\right)^2 - 4[E][I]}}{2[E]} \quad (1)$$

The actual value of K_i or K_i* was calculated from the apparent values using the model for competitive inhibition.[18]

Using the following equation, the isomerization constant (K_{isom}),k_5/k_6, can be calculated.[18]

$$\frac{k_5}{k_6} = \frac{Ki - Ki^*}{Ki^*} \quad (2)$$

All data were fitted to kinetic models using Graphpad Prism.

Statistical Analysis

K_is and IC_{50}s were analyzed for significance using one way ANOVAs with a Tukey's post hoc test and also with Student's *t*-test. Curves were further differentiated by comparing best fit values for IC_{50} to selected data sets using an F-test. Correlations were calculated using Spearman's correlation. All statistical analysis was performed with Graphpad Prism.

Acknowledgment. We thank the Alliance for better Bone Health (Procter and Gamble Pharmaceuticals and Sanofi-Aventis) for financial support of this work through an educational grant. The Structural Genomics Consortium is a registered charity (Number 1097737) that receives funds from the Canadian Institutes for Health Research, the Canadian Foundation for Innovation, Genome Canada through the Ontario Genomics Institute, GlaxoSmithKline, Karolinska Institutet, the Knut and Alice Wallenberg Foundation, the Ontario Innovation Trust, the Ontario Ministry for Research and Innovation, Merck and Co., Inc., the Novartis Research Foundation, the Swedish Agency for Innovation Systems, the Swedish Foundation for Strategic Research, and the Wellcome Trust.

References

(1) Hosking, D.; Lyles, K.; Brown, J. P.; Fraser, W. D.; Miller, P.; Curiel, M. D.; Devogelaer, J. P.; Hooper, M.; Su, G.; Zelenakas, K.; Pak, J.; Fashola, T.; Saidi, Y.; Eriksen, E. F.; Reid, I. R. Long-term control of bone turnover in Paget's disease with zoledronic acid and risedronate. *J. Bone Miner. Res.* **2007**, *22* (1), 142–8.

(2) Coleman, R. E. Bisphosphonates in breast cancer. *Ann. Oncol.* **2005**, *16* (5), 687–95.

(3) Cosman, F.; Borges, J. L.; Curiel, M. D. Clinical evaluation of novel bisphosphonate dosing regimens in osteoporosis: the role of comparative studies and implications for future studies. *Clin. Ther.* **2007**, *29* (6), 1116–27.

(4) Russell, R. G. G.; Xia, Z.; Dunford, J.; Oppermann, U.; Kwaasi, A.; Hulley, P.; Kavanagh, K.; Triffitt, J.; Phipps, R.; Lundy, M.; Barnett, B.; Coxon, F.; Rogers, M.; Watts, N.; Ebetino, F. Bisphosphonates. An Update on Mechanisms of Action and How These Relate to Clinical Efficacy. In *Skeletal Biology and Medicine*; Zaidi, M., Ed.;Annals of New York Academy of Sciences: New York, 2007; Vol. 1117, pp 209–257.

(5) Dunford, J. E.; Thompson, K.; Coxon, F. P.; Luckman, S. P.; Hahn, F. M.; Poulter, C. D.; Ebetino, F. H.; Rogers, M. J. Structure-activity relationships for inhibition of farnesyl diphosphate synthase in vitro and inhibition of bone resorption in vivo by nitrogen-containing bisphosphonates. *J. Pharmacol. Exp. Ther.* **2001**, *296* (2), 235–42.

(6) Bergstrom, J. D.; Bostedor, R. G.; Masarachia, P. J.; Reszka, A. A.; Rodan, G. Alendronate is a specific, nanomolar inhibitor of farnesyl diphosphate synthase. *Arch. Biochem. Biophys.* **2000**, *373* (1), 231–41.

(7) Yardley, V.; Khan, A. A.; Martin, M. B.; Slifer, T. R.; Araujo, F. G.; Moreno, S. N.; Docampo, R.; Croft, S. L.; Oldfield, E. In vivo activities of farnesyl pyrophosphate synthase inhibitors against Leishmania donovani and Toxoplasma gondii. *Antimicrob. Agents Chemother.* **2002**, *46* (3), 929–31.

(8) Luckman, S. P.; Coxon, F. P.; Ebetino, F. H.; Russell, R. G.; Rogers, M. J. Heterocycle-containing bisphosphonates cause apoptosis and inhibit bone resorption by preventing protein prenylation: evidence from structure-activity relationships in J774 macrophages. *J. Bone Miner. Res.* **1998**, *13* (11), 1668–78.

(9) Fisher, J. E.; Rogers, M. J.; Halasy, J. M.; Luckman, S. P.; Hughes, D. E.; Masarachia, P. J.; Wesolowski, G.; Russell, R. G.; Rodan, G. A.; Reszka, A. A. Alendronate mechanism of action: geranylgeraniol, an intermediate in the mevalonate pathway, prevents inhibition of osteoclast formation, bone resorption, and kinase activation in vitro. *Proc. Natl. Acad. Sci. U.S.A.* **1999**, *96* (1), 133–8.

(10) Kavanagh, K. L.; Guo, K.; Dunford, J. E.; Wu, X.; Knapp, S.; Ebetino, F. H.; Rogers, M. J.; Russell, R. G.; Oppermann, U. The molecular mechanism of nitrogen-containing bisphosphonates as antiosteoporosis drugs. *Proc. Natl. Acad. Sci. U.S.A.* **2006**, *103* (20), 7829–34.

(11) Rondeau, J. M.; Bitsch, F.; Bourgier, E.; Geiser, M.; Hemmig, R.; Kroemer, M.; Lehmann, S.; Ramage, P.; Rieffel, S.; Strauss, A.; Green, J. R.; Jahnke, W. Structural basis for the exceptional in vivo efficacy of bisphosphonate drugs. *ChemMedChem* **2006**, *1* (2), 267–73.

(12) Gabelli, S. B.; McLellan, J. S.; Montalvetti, A.; Oldfield, E.; Docampo, R.; Amzel, L. M. Structure and mechanism of the farnesyl diphosphate synthase from *Trypanosoma cruzi*: Implications for drug design. *Proteins* **2006**, *62* (1), 80–8.

(13) Hosfield, D. J.; Zhang, Y.; Dougan, D. R.; Broun, A.; Tari, L. W.; Swanson, R. V.; Finn, J. Structural basis for bisphosphonate-mediated inhibition of isoprenoid biosynthesis. *J. Biol. Chem.* **2004**, *279* (10), 8526–9.

(14) Tarshis, L. C.; Yan, M.; Poulter, C. D.; Sacchettini, J. C. Crystal structure of recombinant farnesyl diphosphate synthase at 2.6-A resolution. *Biochemistry* **1994**, *33* (36), 10871–7.

(15) GeddesA. D. D'SouzaS. M. EbetinoF. H. IbbotsonK. J. *Bisphosphonates: Stucture-activity relationships and therapeutic implication*; Elsevier Science BV: New York, 1994; Vol. 8.

(16) Poulter, C. D.; Rilling, H. Prenyltransferase: The mechanism of the reaction. *Biochemistry* **1976**, *15* (5), 1079–1083.
(17) Martin, M. B.; Arnold, W.; Heath, H. T., 3rd; Urbina, J. A.; Oldfield, E. Nitrogen-containing bisphosphonates as carbocation transition state analogs for isoprenoid biosynthesis. *Biochem. Biophys. Res. Commun.* **1999**, *263* (3), 754–8.
(18) Copeland, R. A. *Enzymes: A Practical Guide to Structure, Mechanism, and Data Analysis*, 2nd ed.; John Wiley & Sons: New York, 2000.
(19) Morrison, J. F.; Walsh, C. T. The behavior and significance of slow-binding enzyme inhibitors. *Adv. Enzymol. Relat. Areas Mol. Biol.* **1988**, *61*, 201–301.
(20) Mao, J.; Mukherjee, S.; Zhang, Y.; Cao, R.; Sanders, J. M.; Song, Y.; Zhang, Y.; Meints, G. A.; Gao, Y. G.; Mukkamala, D.; Hudock, M. P.; Oldfield, E. Solid-state NMR, crystallographic, and computational investigation of bisphosphonates and farnesyl diphosphate synthase-bisphosphonate complexes. *J. Am. Chem. Soc.* **2006**, *128* (45), 14485–97.
(21) Ebetino, F. H.; Dansereau, S. M. Bisphosphonate antiresorptive structure−activity relationships. In *Bisphosphonate on Bones*; Bijvoet, O. L. M., Fleisch, H. A., Cranfield, R. E., Russell, R. G. G., Eds.; Elsevier Science & Technology: Amsterdam, 1995; pp 139–153.
(22) van Beek, E. R.; Cohen, L. H.; Leroy, I. M.; Ebetino, F. H.; Lowik, C. W.; Papapoulos, S. E. Differentiating the mechanisms of antiresorptive action of nitrogen containing bisphosphonates. *Bone* **2003**, *33* (5), 805–11.
(23) Koyama, T.; Tajima, M.; Sano, H.; Doi, T.; Koike-Takeshita, A.; Obata, S.; Nishino, T.; Ogura, K. Identification of significant residues in the substrate binding site of *Bacillus stearothermophilus* farnesyl diphosphate synthase. *Biochemistry* **1996**, *35* (29), 9533–8.
(24) Song, L.; Poulter, C. D. Yeast farnesyl-diphosphate synthase: Site-directed mutagenesis of residues in highly conserved prenyltransferase domains I and II. *Proc. Natl. Acad. Sci. U.S.A.* **1994**, *91* (8), 3044–8.
(25) Evdokimov, A.; Pokross, M.; Barnett, B. L.; Kavanagh, K.; Oppermann, U.; Russell, R. G. G.; McKenna, C. E.; Ebetino, F. H. Human farnesyl diphosphate synthase crystal structures with active and inactive bisphosphonates. *Bone* **2006**, *38* (Issue 3, Supplement 1), 49.
(26) Yin, F.; Cao, R.; Goddard, A.; Zhang, Y.; Oldfield, E. Enthalpy versus entropy-driven binding of bisphosphonates to farnesyl diphosphate synthase. *J. Am. Chem. Soc.* **2006**, *128* (11), 3524–5.
(27) Ebetino, F. H. Elucidation of a pharmacophore for the bisphosphonate mechanism of bone antiresorptive activity. *Phosphorus, Sulfur Silicon Relat. Elem.* **1996**, *109* (1), 217.
(28) Reed, B. C.; Rilling, H. C. Substrate binding of avian liver prenyltransferase. *Biochemistry* **1976**, *15* (17), 3739–45.
(29) Wiliams, J. W.; Morrison, J. F. The kinetics of reversible tight-binding inhibition. *Methods Enzymol.* **1979**, *63*, 437–467.
(30) Morrison, J. F. Kinetics of the reversible inhibition of enzyme-catalysed reactions by tight-binding inhibitors. *Biochim. Biophys. Acta* **1969**, *185* (2), 269–86.
(31) Rogers, M. J.; Xiong, X.; Brown, R. J.; Watts, D. J.; Russell, R. G.; Bayless, A. V.; Ebetino, F. H. Structure−activity relationships of new heterocycle-containing bisphosphonates as inhibitors of bone resorption and as inhibitors of growth of *Dictyostelium discoideum* amoebae. *Mol. Pharmacol.* **1995**, *47* (2), 398–402.
(32) Fleisch, H.; Russell, R. G.; Francis, M. D. Diphosphonates inhibit hydroxyapatite dissolution in vitro and bone resorption in tissue culture and in vivo. *Science* **1969**, *165* (899), 1262–4.

JM7015733